

CHEMISTRY

AN **ASIAN** JOURNAL

www.chemasianj.org

Accepted Article

Title: Stimuli-responsive Metallogels for synthesizing Ag nanoparticles and Sensing Hazardous Gases

Authors: Parthasarathi Dastidar, Protap Biswas, and Sumi Ganguly

This manuscript has been accepted after peer review and appears as an Accepted Article online prior to editing, proofing, and formal publication of the final Version of Record (VoR). This work is currently citable by using the Digital Object Identifier (DOI) given below. The VoR will be published online in Early View as soon as possible and may be different to this Accepted Article as a result of editing. Readers should obtain the VoR from the journal website shown below when it is published to ensure accuracy of information. The authors are responsible for the content of this Accepted Article.

To be cited as: *Chem. Asian J.* 10.1002/asia.201800743

Link to VoR: <http://dx.doi.org/10.1002/asia.201800743>

A Journal of



A sister journal of *Angewandte Chemie*
and *Chemistry – A European Journal*

WILEY-VCH

Stimuli-responsive Metallogels for synthesizing Ag nanoparticles and Sensing Hazardous Gases

Protap Biswas, Sumi Ganguly, and Parthasarathi Dastidar*^[a]

Dedication ((optional))

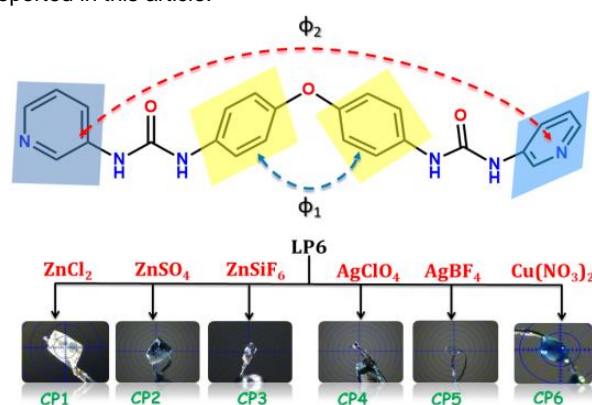
Abstract: A newly synthesized bis-pyridyl ligand having a diphenyl ether backbone (**LP6**) displayed the ability to form crystalline coordination polymers (**CP1-CP6**) which were fully characterized by single crystal X-ray diffraction and most of them turned out to be lattice occluded crystalline solids – a structural characteristic reminiscent to gels. The reactants of the coordination polymers produced metallogels in DMSO/water confirming the validity of the design aspect based on which the coordination polymers were synthesized. Some of the metallogels displayed material properties like in situ synthesis of Ag nanoparticles and stimuli-responsive gel-sol transition including sensing hazardous gases like ammonia and hydrogen sulphide.

Introduction

Research on supramolecular gels has gained much impetus in the quest for developing new functional materials.^[1-16] Various materials applications such as light harvesting,^[17] catalysis^[18-20] structure-directing agents,^[21-22] synthesis of nanoparticles,^[23-26] dye adsorption,^[27-29] containing oil spill,^[30,31] art conservation,^[32-33] sensing,^[34-36] drug delivery,^[37-40] tissue engineering^[41-42] etc. are now feasible with supramolecular gels. Metallogel is a special type of supramolecular gel wherein metal-ligand coordination takes an important part in gelation.^[43] It is now well accepted that during gelation, the gelator molecules self-assemble via various intermolecular interactions such as π - π -stacking, H-bonding, van der Waals interactions, halogen bonding etc. to form self-assembled-fibrillar-networks (SAFINs) – a 3D network within which the solvent molecules are immobilized to result a gel. In metallogel, metal-ligand coordination along with other noncovalent interactions facilitates the formation of SAFIN. Metallogelation is reported to be exerted by random coordination polymers,^[44-45] hyper-branched coordination polymers,^[46] coordination complexes^[47-49] etc. Designing gelators is a challenging task because exact details of molecular level gelation mechanism are still unclear. Nevertheless, there have been efforts by various groups to

design metallogelators.^[50-55] We^[56-58] and others^[59] reasoned that a large amount of solvent molecules were entrapped within the gel network akin to what was observed in a lattice occluded molecular solid (LOMS). Thus, the compounds having structural characteristics to form LOMS may possess promising potential as gelators under suitable conditions. In fact, we have successfully designed coordination polymer based metallogelators by exploiting such structural aspects.^[60-62]

We have synthesized a new bis-pyridyl-bis-urea ligand namely [1,1-(oxybis(4,1-phenylene))bis(3-(pyridine-3-yl)urea)] (**LP6**) and reacted with various metal (Zn(II), Cu(II) and Ag(I)) salts (1:1 molar ratio) with the aim of developing coordination polymer based metallogelators. Due to the extended coordination involving the pyridyl N of **LP6** and the metal center, such reactions are expected to produce 1D coordination polymers. The bis-urea backbone of **LP6** is likely to act as H-bonding sites that might help occlude solvent molecules within the crystal lattice as well as provide important inter-chain interactions required for growing the gel network. Thus, under suitable conditions, **LP6** and metal salts should produce metallogels. We have successfully isolated six coordination polymers (**CP1-CP6**) by reacting **LP6** with various metal salts, characterized them using single crystal X-ray diffraction (SXRD) and other physicochemical techniques (Scheme 1). Reactants of all the **CPs**, except **CP3**, provided metallogels in DMSO/water. Details of the structure-property correlation of these metallogels and their various applications such as nanoparticle synthesis, stimuli responsive gel-sol transition, sensing of hazardous gases are reported in this article.



Scheme 1. Chemical structure of **LP6** and the optical micrograph of the single crystals of **CP1-CP6**.

Results and Discussion

The bis-pyridyl-bis-urea ligand **LP6** was synthesized following literature procedure^[63] (see experimental). Single

[a] P. Biswas, S. Ganguly, Prof. P. Dastidar
Department of Organic Chemistry
Indian Association for the Cultivation of Science. (IACS)
2A and 2B, Raja S. C. Mullick Road Jadavpur, Kolkata, 700032,
West Bengal (India)
Fax: (+91) 33-2473-2805
E-mail: ocpd@iacs.res.in

Supporting information for this article is given via a link at the end of the document. *(Please delete this text if not appropriate)*

crystals of the ligand were grown by slow evaporation from DMF/acetonitrile (2:3 v/v) and one such single crystal was subjected to SXRD (Table 1).

<<Table 1 is appended at the end of this document>>

Crystal structure of LP6. The crystal of LP6 belonged to the noncentric monoclinic space group $P2_1$. The asymmetric unit comprised two crystallographically independent molecules (designated as LP6a and LP6b); both the molecules displayed V-shaped conformation having significantly different dihedral angle involving the central phenyl rings ($\Phi_1 = 73.8^\circ$ and 89.3°) and terminal pyridyl moieties ($\Phi_2 = 44.1^\circ$ and 42.8°). The molecular axis of both the molecules in the asymmetric unit coincided with the long axis i.e. the b-axis of the unit cell. In the asymmetric unit, LP6a and LP6b were held together through H-bonding involving the urea moieties; while one of the urea moieties of LP6a formed typical bifurcated H-bonding of urea with LP6b, the other urea functionality of LP6a displayed H-bonding with urea $>C=O$ of LP6b and neighbouring LP6a molecule via N-H...N interactions involving one of the terminal pyridyl N resulting in an overall 2D hydrogen bonded network that propagated parallel to a-c plane (Figure 1).

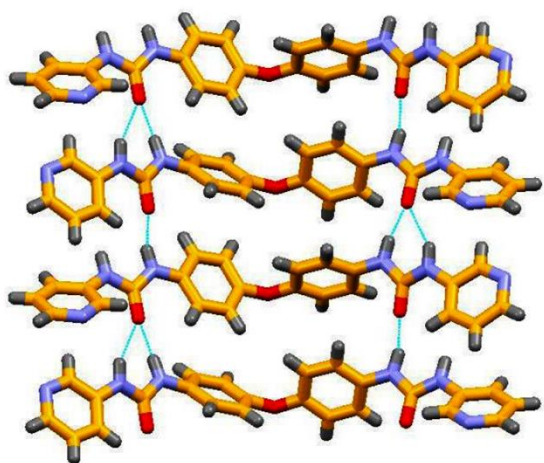
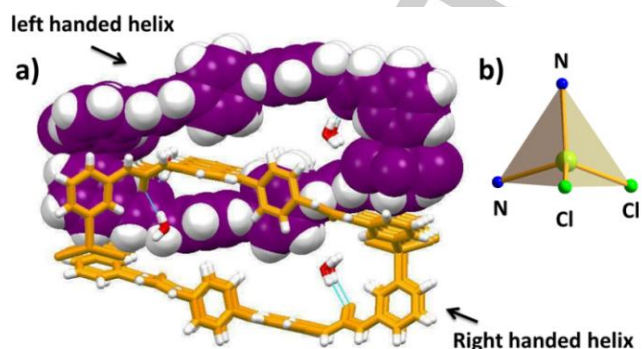


Figure 1. Crystal structure illustration of LP6: assembly of the ligand molecules involving hydrogen bonding among urea moieties.

The coordination polymers (CP1-CP6) were synthesized by slow evaporation method that produced X-ray quality single crystals (details in the experimental section). All these crystals were subjected SXRD (Table 1).

Crystal structure of CP1. The space group assigned to CP1 was the centrosymmetric orthorhombic $Pca2_1$. In the asymmetric unit are located one ligand molecule, one $ZnCl_2$ and one lattice occluded solvate water molecule. The conformation of LP6 molecule was characterized by $\Phi_1 = 86.6^\circ$ and $\Phi_2 = 56.4^\circ$. In the crystal structure, both right- and left-handed helical 1D

coordination polymer chains (generated due to the extended N-Zn coordination involving the ligand and tetrahedral Zn(II) metal center) were found to be intercalated via N-H...O H-bonding involving the urea moieties of the neighbouring chains as well as

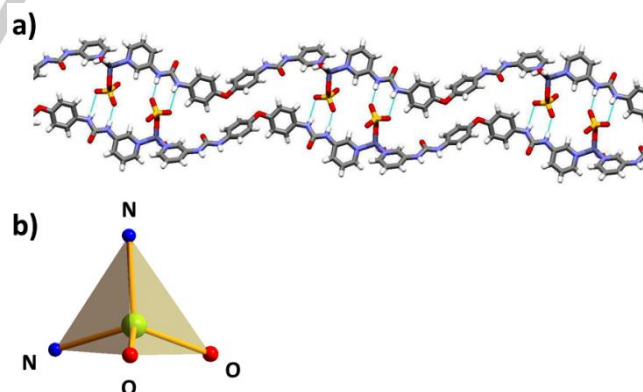


lattice occluded water and urea functionality of the chains (Figure 2).

Figure 2. Crystal structure illustration of CP1; a) intertwined right and left handed helical polymer chains (top view); b) tetrahedral coordination geometry of Zn(II)

Crystal structure of CP2.

The crystal of CP2 belonged to the centrosymmetric triclinic space group $P-1$. In the asymmetric unit, one LP6 ligand, one sulfate anion and one water molecule were found to be coordinated with the tetrahedral Zn(II) metal center. The characteristic dihedral angles in LP6 were $\Phi_1 = 77.1^\circ$ and $\Phi_2 = 54.1^\circ$. Extended coordination involving the terminal pyridyl moiety of LP6 and Zn(II) resulted in 1D coordination polymer chains which were packed in parallel fashion sustained by



typical urea...sulfate synthon, O-H...O H-bonding involving sulfate, and metal bound water molecule (Figure 3).

Figure 3. Crystal structure illustration of CP2; a) self-assembly of two parallel 1D polymer chain displaying urea-sulfate synthon; b) tetrahedral coordination geometry of Zn(II)

Crystal structure of CP3. The crystal of **CP3** crystallized in the noncentric triclinic space group $P1$. The asymmetric unit comprised two fully occupied **LP6** molecules coordinated to Zn(II) metal center, two metal bound water, one uncoordinated SiF_6^{2-} counter ion, and two water and one methanol molecules as lattice occluded guests. The characteristic dihedral angles in **LP6** were $\Phi_1 = 78.8^\circ/81.7^\circ$ and $\Phi_2 = 48.3^\circ/77.5^\circ$. Interestingly, Zn(II) metal center displayed rarely observed trigonal bipyramidal coordination geometry^[64] wherein the equatorial sites were coordinated by pyridyl N of **LP6** and the apical positions were occupied by water molecules. Due to extended coordination exerted by the terminal pyridyl N of one of the **LP6** molecules in the asymmetric unit a 1D polymer chain was formed wherein the other **LP6** molecule was found to be coordinated via pyridyl N-Zn(II) keeping the other pyridyl N free from coordination. The 1D polymer chains were packed in parallel fashion along the a-axis. The guest molecules were found to be stabilized within the crystal lattice via O-H...O and N-H...O H-bond interactions (Figure 4).

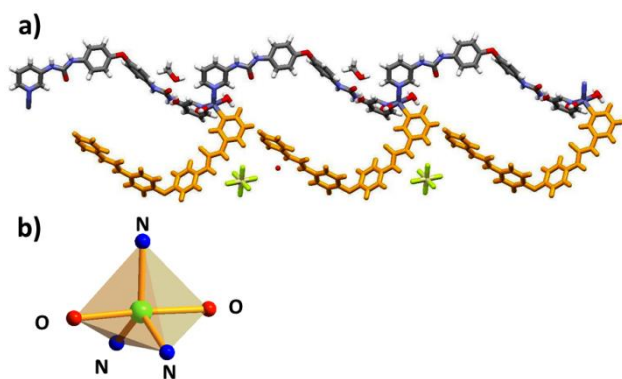


Figure 4. Crystal structure illustration of **CP3**; a) 1D polymer chain displaying anchored **LP6** molecules via mono-coordination; b) rarely observed trigonal bipyramidal coordination geometry of Zn(II).

Crystal structure of CP4. The crystal of **CP4** belonged to the centrosymmetric monoclinic space group $C2/c$. In the asymmetric unit, one **LP6** molecule, one Ag(I) metal ion and two half occupied ClO_4^- counter ions curiously disordered around symmetry elements were located; while one ClO_4^- was located on a center of inversion, the other one was disordered around $C2$ axis. The characteristic dihedral angles in **LP6** were $\Phi_1 = 85.5^\circ$ and $\Phi_2 = 57.3^\circ$. The metal center Ag(I) displayed nearly linear coordination geometry ($\angle \text{N-Ag-N} = 172.4^\circ$); the disordered counter ions appeared to be weakly coordinated to the metal center ($\text{Ag-O} = 2.578\text{-}3.103 \text{ \AA}$). In the crystal structure, 1D polymer chains were formed due to the extended coordination of the bidentate ligand **LP6** with Ag(I) metal center; such 1D chains were arranged in crisscross manner sustained by one of the disordered counter ions which acted as a bridge between the chains via Ag-O coordination (Ag

$\text{O} = 2.578 \text{ \AA}$) resulting in 2D sheets packed parallel to b-c plane (Figure 5).

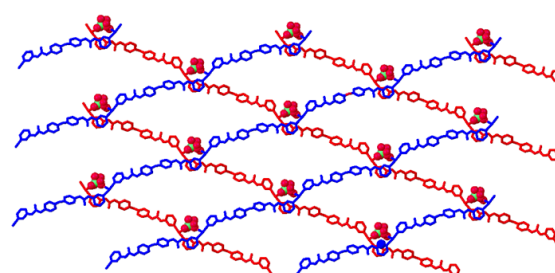


Figure 5. Crystal structure illustration of **CP4**; 2D sheet formed via counter anion bridging with the crisscross array of 1D polymer chains.

Crystal structure of CP5. The crystal of **CP5** belonged to the centrosymmetric triclinic space group $P-1$. In the asymmetric unit, one **LP6**, one Ag(I) metal ion, one BF_4^- , one metal bound DMF and one lattice occluded DMF were located. The characteristic dihedral angles in **LP6** were $\Phi_1 = 73.6$ and $\Phi_2 = 56.7$. The bidentate ligand **LP6** was involved in extended N-Ag(I) coordination resulting in 1D polymer chain. The Ag(I) was found to be trigonally coordinated wherein opposite sites were coordinated by pyridyl N of **LP6** ($\angle \text{N-Ag-N} = 164.4^\circ$) and the remaining site was coordinated by O of DMF ($\text{Ag-O} = 2.684 \text{ \AA}$). The 1D chains were packed in parallel fashion. The lattice occluded solvent DMF was found to be stabilized in the crystal lattice via N-H...O bifurcated H-bonding (Figure 6).

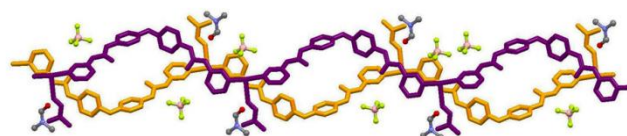


Figure 6. Crystal structure illustration of **CP5**; parallel arrangement of 1D polymer chains.

Crystal structure of CP6. Interestingly, **CP6** crystallized in the noncentric tetragonal space group $P4_2$. In the asymmetric unit, two fully occupied **LP6** – each coordinated to two crystallographically independent half occupied Cu(II) metal ions, four half occupied metal bound water molecules, two fully occupied nitrate counter ions and five fully occupied lattice occluded water molecules were located. The characteristic dihedral angles in **LP6** molecules were $\Phi_1 = 81.9^\circ, 61.6^\circ$ and $\Phi_2 = 86.2^\circ, 79.0^\circ$. Extended coordination of the **LP6** molecules with the metal center generated 1D polymer having looped chain topology. Relatively large void space of the loops ($\sim 15.5 \times 16.7 \text{ \AA}$) were occupied by 2-fold interpenetration by another looped chain polymer and such 2-fold interpenetrated polymer chains were packed in parallel fashion along c-axis. The counter ions nitrate and solvate water molecules were located

within the interstitial space stabilized by various O-H...O and N-H...O hydrogen bonding (Figure 7).

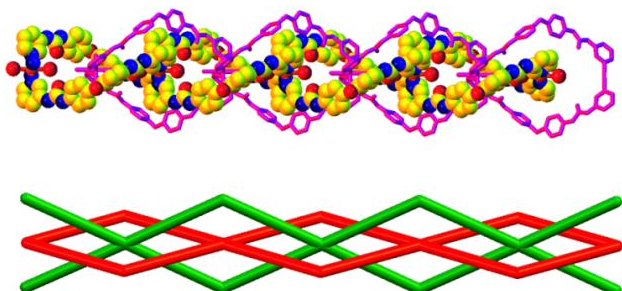


Figure 7. Crystal structure illustration of **CP6**; top-2-fold interpenetrated 1D looped chain; bottom- TOPOS.^[65-66] representation of the interpenetrated chains.

Comparison of powder X-ray diffraction (PXRD) patterns (both simulated from SXRD data and experimental PXRD on bulk solids) of the CPs revealed that in majority of the cases, most of the major peaks were near superimposable indicating excellent crystalline phase purity (see the Supporting Information, Figure S21-27). The bis-pyridyl ligand **LP6** being flexible owing to C-N and C-O bond rotation displayed various conformations in the crystal structures of **LP6** and its coordination polymers as characterized by different dihedral angles Φ_1 and Φ_2 . While the free ligand **LP6** displayed monoclinic crystal system having chiral space group ($P2_1$), the majority of the CPs (**CP2**, **CP3** and **CP5**) crystallized in the triclinic space groups ($P1$ and $P-1$); the rests (**CP1**, **CP4** and **CP6**) showed orthorhombic ($Pca2_1$), monoclinic ($C2/c$) and tetragonal ($P4_2$) crystal systems. Since majority of the CPs (except **CP2** and **CP4**) displayed lattice inclusion phenomenon in the crystal structures, they may be suitable for gelation studies as envisaged (see above).

Gelation studies. The free ligand **LP6** having urea and pyridyl functionalities was expected to give gels; however, being nearly insoluble in any organic solvents other than DMF and DMSO, it failed to show any gelation property from a pure solvent. Aqueous solution of **LP6** in DMSO/water (2:3 v/v) produced gelatinous precipitate, the SEM image of which displayed aggregated spherical particles instead of fibers typically observed for supramolecular gels (see the Supporting Information, Figure S18). To obtain metallo gels, we reacted **LP6** with the corresponding metal salts in 1:1 molar ratio as we have reacted the ligand and the corresponding metal salts in the same ratio while attempting the synthesis of the CPs. In a typical experiment, **LP6** (10 mg) was taken in DMSO (0.4 mL) and slowly added to an aqueous solution (0.6 mL) of metal salt (equimolar amount) at room temperature. In all the cases, gels were formed instantaneously. Following this method, we obtained metallo gels namely **CPMG1**, **CPMG2**, **CPMG4**, **CPMG5**,

CPMG6 corresponding to all the CPs except **CP3**; in this case, a gelatinous precipitate was observed. Interestingly, metallo gel (**MG7**) was also obtained from **LP6** and CuCl_2 in DMSO/water (2:3 v/v) after 7-8 h at room temperature. It was also observed that some chloride salts did have the tendency to form metallo gels with **LP6**. Thus, metallo gels were obtained by reacting **LP6** with various metal chloride salts (MnCl_2 , CdCl_2 , CoCl_2 and NiCl_2). Remarkably, even NaCl also produced metallo gels under the similar conditions (Figure 8, Table 2).

<<Table 2 is appended at the end of this document>>

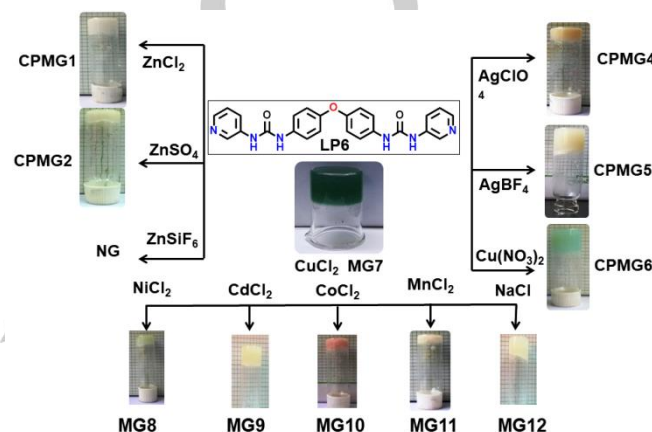


Figure 8. Various metallo gels obtained from DMSO:H₂O (2:3)

All the gels except **MG7** were not thermo-reversible indicating coordination polymer nature of the gel network; **MG7**, however, was thermo-reversible ($T_{\text{gel}} = 50^\circ\text{C}$, at

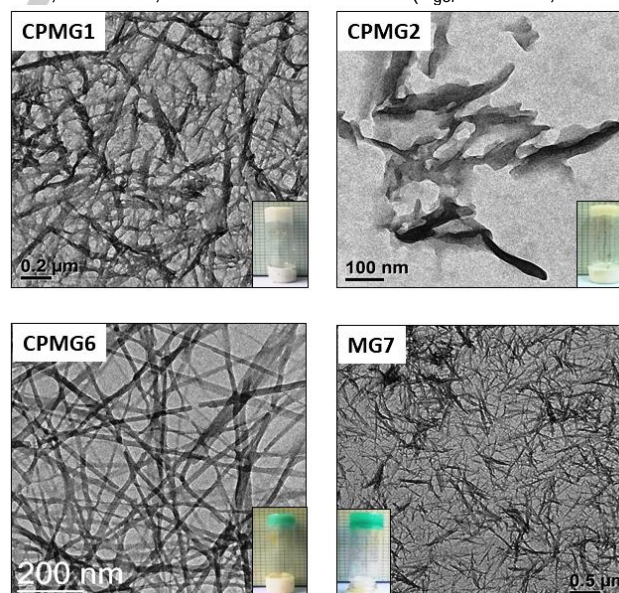


Figure 9. HRTEM images of the xerogels; inset – optical images of the corresponding gels in DMSO/water.

MGC). Interestingly, beyond 60 °C, **MG7** displayed permanent phase separation with a colour change from bluish-green to greenish-yellow. Efforts to grow single crystals from the reaction mixtures of **MG7-MG12** under various conditions were not successful. Therefore, in the absence of the crystal structures of **MG7-MG12**, it is difficult to comment on the plausible structural features of the corresponding gel networks.

To study the morphology of the gel network, we carried out high resolution transmission electron microscopy on the xerogels derived from **CPMG1**, **CPMG2**, **CPMG4**, **CPMG5**, **CPMG6** and also **MG7**; typical highly entangled fibrous morphology was obtained in the cases **CPMG1**, **CPMG6** and **MG7** whereas tape like morphology was observed for **CPMG2** (Figure 9).

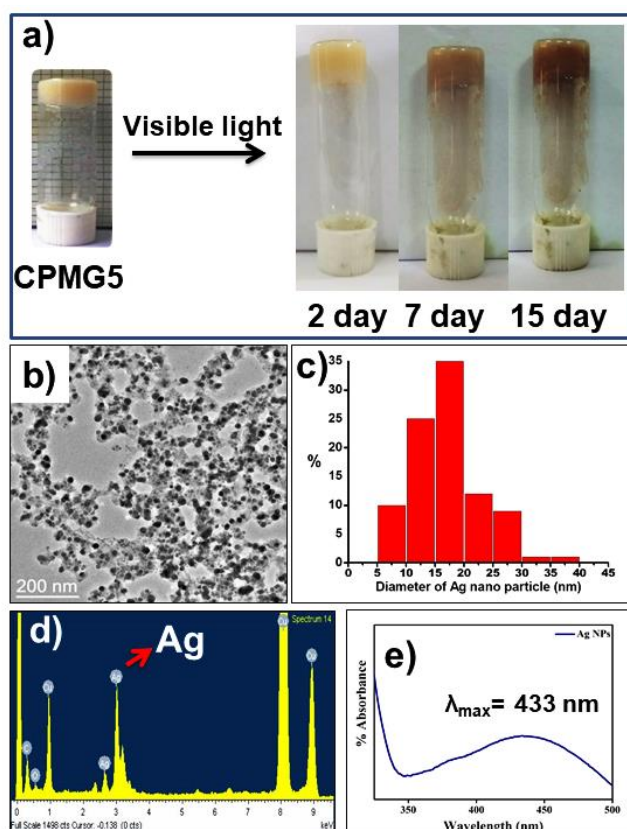


Figure 10. Ag nanoparticle in Gel bed: a) time dependent formation of Ag nanoparticles; b) TEM image of the aged xerogel (15 days) displaying Ag nanoparticles anchored to the gel network; c) size distribution of Ag nanoparticles as observed in TEM image; d) EDAX spectra confirming the presence of Ag in TEM sample; e) typical surface plasmon resonance spectra of the Ag nanoparticles.

The metallogels derived from Ag(I) i.e. **CPMG4** and **CPMG5** displayed darkening of its colour (towards dark brown) when exposed to visible light at room temperature; while **CPMG4** collapsed to sol after 3-4 days exposure, **CPMG5** remained intact for more than a month. TEM images of the dried

samples of these light exposed metallogels revealed the existence of Ag nanoparticles (~20 nm) adhered to the fibrous network. Ag nanoparticle containing gel suspended in DMSO showed the typical surface plasmon spectra ($\lambda_{\max} = 433$ nm) in UV-vis. Such observations of Ag nanoparticle formation from Ag(I) CP based metallogels were reported by us^[67] and others.^[68-70] (Figure 10).

Whether a material is gel or not is confirmed by its visco-elastic (gel like) response in dynamic rheology (frequency sweep) wherein viscous modulus (G') and loss modulus (G'') are plotted against frequency (ω , rad/s); $G' > G''$ along with frequency invariance of G' over the entire frequency range (ω , rad/s) is observed typically for a gel.^[71] Thus, visco-elastic nature of the metallogels was studied by dynamic rheology. We performed frequency sweep experiments with 10 wt % gels in 2:3 DMSO/water at a strain of 0.1 % as suggested by the amplitude sweep experiments (see the Supporting Information, Figure S33). Data revealed that majority of the metallogels displayed excellent visco-elastic response; G' 's were found to be much larger than G'' ($G'/G'' = 0.04-0.23$) and were nearly frequency invariant (Table 3). Therefore, the visco-elastic (gel) properties of these metallogels were established (Figure 11).

<<Table 3 is appended at the end of this document>>

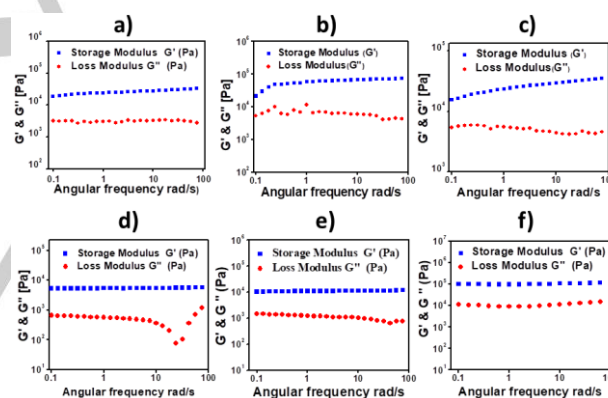


Figure 11. Rheological behaviour of the metallogels; a) **CPMG1** b) **CPMG2** c) **CPMG4** d) **CPMG5** e) **CPMG6** f) **MG7**

We also compared PXRD patterns of the CPs under various conditions (simulated and xerogel) in order to study whether the network structure of the xerogel remained the same as observed in the corresponding single crystal structure or not. (see the Supporting Information, Figure S28-32) revealed that all the major peaks in the cases of **CP1**, **CP2** and **CP6** corresponded well indicating that in these cases, the xerogel network indeed remained intact. On the other hand, the PXRDs of the xerogels for **CP4** and **CP5** were poorly crystalline which was attributed to the formation of Ag nanoparticles thereby disrupting the xerogel networks in these cases.

Stimuli responsive gels are important class of smart materials that can sense various changes in its environment and display interesting transitions (gel-sol in response to heat, light energy, mechanical stress, pH change etc., colour change, swelling-contraction etc.) that can have various potential applications.^[72-74] Since **MG7** is the only thermoreversible metallogel reported herein, we considered exploring its response against various stimuli. Thus, a sample of **MG7** metallogel (1 mL, 4.5 wt % in 2:3 DMSO/water) at 50 °C readily formed sol which upon cooling to room temperature produced gel and such thermoreversible phase transition could be continued for a few cycles. Thixotropic behavior of the metallogel was also evident; mechanical stress (shaking by hand) resulted in sol which, upon rest for just 10 mins produced the gel. Thixotropic behaviour was also supported by dynamic rheology wherein **MG7** displayed typical rheo-reversible feature (see the supporting information, Figure S34). Reversible gel-sol transition was also achieved by redox stimulus; the metallogel transformed to yellow sol when treated with a reducing agent like ascorbic acid (15 μ L, 1M solution in water); the sol was readily transformed to gel by treating with required amount of H_2O_2 (~50 μ L, 30% aqueous solution). Understandably, ascorbic acid was able to reduce Cu(II) to Cu(I) thereby disrupting the network resulting in sol, which upon treatment with H_2O_2 must have oxidized Cu(I) to Cu(II) thereby regaining the network structure that resulted in gelation. Aqueous ammonia (10 μ L, 25 % in water) was also capable of inducing gel to sol transition; deep blue colour of the sol clearly indicated ammonia-Cu(II) coordination. The sol (deep blue) readily transformed to green gel when acidified with 1N HCl or sky blue gel when treated with glacial acetic acid (Figure 12).

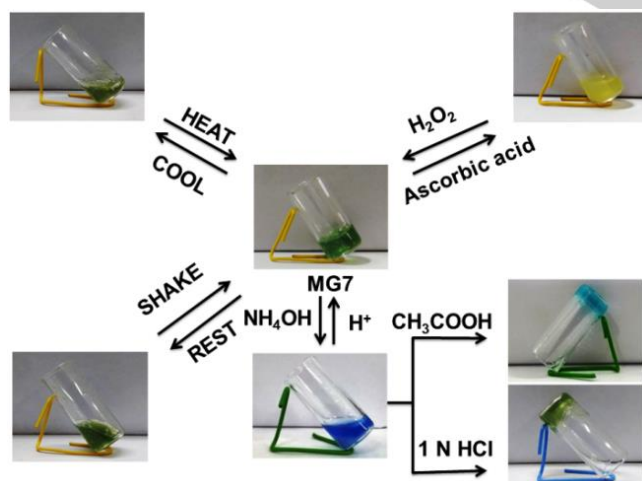


Figure 12. Stimuli-responsive behaviour of **MG7**.

Half an hour exposure to ammonia vapour or H_2S gas also induced gel to sol transition indicating its ability to sense

such hazardous gases. Both ammonia and H_2S have the ability to coordinate to the metal center thereby disrupting the gel network leading to gel-sol transition (Figure 13).

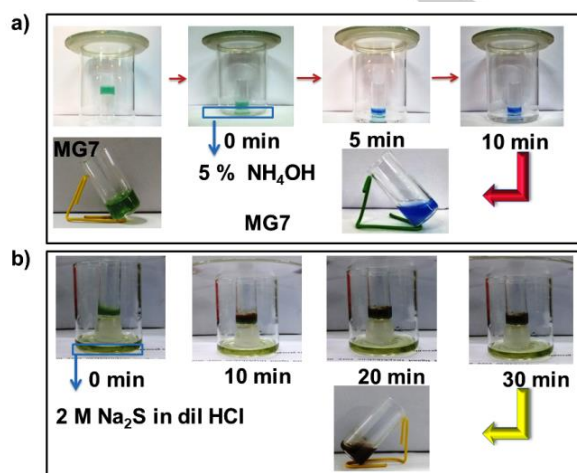


Figure 13. Stimuli-responsive sensing of hazardous gases by **MG7**

Conclusions

Thus, we demonstrated that the coordination polymers designed and synthesized did possess lattice occluded solvent molecules as envisaged; while extended coordination involving the pyridyl N and metal ion guaranteed the formation of coordination polymeric network, the bis-urea functionality of the ligand **LP6** ensured self-assembly of the polymeric chains via hydrogen bonding and helped occlude solvent molecules as guests in majority cases; except **CP2** and **CP4**, all turned out to be lattice occluded crystalline solids that were expected to provide metallogels. Gelation data clearly supported the hypothesis; except for **CP3**, all the other reactants of CPs provided metallogels in DMSO/water (2:3 v/v). Remarkably, the ligand **LP6** provided metallogels with various metal ions displaying preference towards chloride anion for gelation. Interestingly, **CPMG5** produced Ag nanoparticles whereas **MG7** showed interesting stimuli-responsive behavior including sensing of hazardous gases like ammonia and hydrogen sulfide. The results presented herein clearly demonstrated the merit of rational approach based on crystal engineering rationale to design coordination polymer based metallogels for various applications.

Experimental Section

Materials and methods for Physical measurements:

All the chemicals were commercially available and used without further purification. FT-IR spectra were obtained on a FT-IR instrument (FTIR-8300, Shimadzu). The elemental compositions of the purified compounds were confirmed by elemental analysis (Perkin Elmer Precisely, Series-II, CHNO /S Analyser-2400). TGA analyses were performed on a SDT Q

Series 600 Universal VA.2E TA instrument. X-ray powder diffraction patterns were recorded on a Bruker AXS D8 Advance Powder (Cu K α radiation, $\lambda=1.5406 \text{ \AA}$) X-ray diffractometer. TEM images were recorded using a JEOL instrument with 300 mesh copper TEM grid. Scanning electron microscopy (SEM) data was collected in a JEOL, JMS-6700F.UV-Vis spectroscopic measurements were carried out on a Hewlett-Packard 8453 diode array spectrophotometer equipped with a Peltier temperature controller. NMR spectra were recorded using 400 MHz spectrometer (Bruker Ultrashield Plus- 400).

Synthesis of 1,1'-(oxybis(4,1-phenylene))bis(3-(pyridin-3-yl)urea)

LP6: The ligand **LP6** was synthesized following a literature procedure with modification. 3-aminopyridine (1g, 1.0 mmol) and dry triethylamine (3 mL) were dissolved in dry DCM (150 mL) in a round bottom flask (500 mL) by stirring at r.t. under nitrogen atmosphere. The solution was then cooled in an ice bath and solid triphosgene (1g, 0.33 mol) was added to it and stirred for 45 min. under the same condition in order to generate 3-pyridyl isocyanate. 4-4'-oxydianiline (1.06 g, 0.51 mmol) dissolved in dry DCM (50 mL) was added dropwise to the isocyanate solution under the same condition. The reaction mixture was then stirred for 6 h at r.t. followed by reflux for another 6 h at 50 °C. The precipitate thus formed was filtered in a suction pump and stirred in NaHCO $_3$ solution (5%, 100 mL) for overnight. The ligand **LP6** was isolated as white precipitate (Yield: 1.42g, 66.2%) by filtering followed by drying in open air. Single crystals of **LP6** were obtained in DMF/CH $_3$ CN (2:3) in slow evaporation method.

LP6:¹H NMR (400 MHz, [D $_6$] DMSO, 25°C): $\delta=8.803$ (s, 1H), 8.768 (s, 1H), 8.590-8.584 (d, $j=2.4$, 2H), 8.174-8.172 (m, 2H), 7.933-7.911 (m, 2H), 7.426-7.429 (d, $J=12$, 2H), 7.313-7.280 (m, 2H), 6.947-6.924 ppm(d, $J=9$, 2H) (see Supporting Information, Figure S1); ¹³C NMR (100 MHz, [D $_6$] DMSO, 25°C): $\delta= 152.674, 152.007, 142.796, 139.981, 136.470, 134.736, 125.152, 123.504, 120.245, 118.796, 117.398$ ppm (see Supporting Information, Figure S2); ESI-MS (MeOH): calculated for [M+H] $^+$ is 441.16, found 441.42 (see Supporting Information, Figure S3). FT-IR (KBr, cm $^{-1}$): $\tilde{\nu}= 3272$ (brs, Urea N-H stretch) 1654 (s, Urea C=O stretch), (see the Supporting Information, Figure S4).

Synthesis of the coordination polymers.

The coordination polymers reported herein were synthesized following layering method. Typically within two weeks, X-ray quality crystals of the CPs were obtained which were subjected to various characterizations including single crystal X-ray diffraction (SXRD).

Synthesis and characterisation of {[Zn(LP6)(Cl) $_2$]-H $_2$ O] $_{\infty}$ (CP1): The coordination polymer **CP1** was synthesised by layering method. **LP6** (44 mg, 0.1 mmol) was taken in DMF (4 mL) and MeOH (9 mL) layered over aqueous solution of ZnCl $_2$ (2mL, 13.6 mg, 0.1 mmol). After one week, colourless, blocked-shaped crystals were obtained. Elemental analysis (calcd (found) %) for C $_{24}$ H $_{22}$ Cl $_2$ N $_6$ O $_4$ Zn: C, 48.47 (48.42), H, 3.73 (3.50), N, 14.13 (14.38) %; FT-IR (KBr, cm $^{-1}$): $\tilde{\nu}= 3295$ (brs, urea N-H stretch), 1715 (s, urea C=O stretch) (see the Supporting Information, Figure S5)

Synthesis and characterisation of the {[Zn(LP6)(SO $_4$)]-H $_2$ O] $_{\infty}$ (CP2):

The coordination polymer **CP2** was synthesised by layering method. **LP6** (44 mg, 0.1 mmol) was taken in DMF (4 mL) and MeOH (9 mL) layered over aqueous solution of ZnSO $_4$ (2 mL, 28.7mg, 0.1 mmol). After two weeks colourless, blocked-shaped crystals were obtained. Elemental analysis calcd (%) for C $_{24}$ H $_{22}$ N $_6$ O $_8$ SZn: C, 46.50 (46.58), H 3.58 (3.51), N, 13.56 (13.49) %; FT-IR (KBr, cm $^{-1}$): $\tilde{\nu}= 3295$ (brs, urea N-H stretch), 1715 (s, urea C=O stretch) (see the Supporting Information, Figure S5).

Synthesis and characterisation of the

{[Zn(LP6) $_2$ (H $_2$ O) $_2$]-SiF $_6$ ·CH $_3$ OH·(H $_2$ O) $_2$] $_{\infty}$ (CP3): The coordination polymer **CP3** was synthesised by layering method. **LP6** (44mg, 0.1 mmol) ligand was taken in DMF (4 mL) and MeOH (9 mL) and layered over aqueous solution of ZnSiF $_6$ (2 mL, 10.3 mg, 0.1 mmol). After four weeks, colourless, blocked-shaped crystals were obtained. Elemental analysis (calcd (found) %) for C $_{49}$ H $_{52}$ F $_6$ N $_12$ O $_11$ SiZn: C, 49.35 (49.46), H, 4.40 (4.32), N, 14.10 (13.90) %; FT-IR (KBr, cm $^{-1}$): $\tilde{\nu}= 3399$ (brs, urea N-H stretch), 1688(s, urea C=O stretch), (see the Supporting Information, Figure S5)

Synthesis characterisation of the {[Ag(LP6)(ClO $_4$)]] $_{\infty}$ (CP4):

The coordination polymer **CP4** was synthesised by layering method. **LP6** (44 mg, 0.1 mmol) was taken in DMF (4 mL), MeOH (9 mL) and layered over aqueous solution of AgClO $_4$ (2 mL, 20.7mg, 0.1 mmol). After two weeks pale colour, block shaped crystals were obtained. Elemental analysis (calcd (found) %) for C $_{24}$ H $_{20}$ AgClN $_6$ O $_7$: C, 44.50 (44.79), H, 3.11 (3.26), N, 12.97 (12.81) %; FT-IR (KBr, cm $^{-1}$): $\tilde{\nu}= 3366$ (brs, urea N-H stretch), 1702 (s, urea C=O stretch), (see the Supporting Information, Figure S5)

Synthesis characterisation of the {[Ag(LP6)(BF $_4$)(DMF)]DMF] $_{\infty}$ (CP5):

The coordination polymer **CP5** was synthesised by layering method. **LP6** (44 mg, 0.1 mmol) was taken in DMF (4 mL), CH $_3$ OH (9 mL) and layered over aqueous solution of AgBF $_4$ (2 mL, 19.7mg, 0.1 mmol). After three weeks pale colour, plate shaped crystals were obtained. Elemental analysis (calcd (found) %) for C $_{27}$ H $_{27}$ AgBF $_4$ N $_7$ O $_4$: C, 45.79 (45.62), H, 3.84 (3.67), N, 13.84 (13.65) %; FT-IR (KBr, cm $^{-1}$): $\tilde{\nu}= 3317$ (brs, urea N-H stretch), 1654 (s, urea C=O stretch), (see the Supporting Information, Figure S5)

Synthesis characterisation of the {[Cu $_2$ (LP6) $_2$ (NO $_3$)(H $_2$ O)](4H $_2$ O)] $_{\infty}$ (CP6):

The coordination polymer **CP6** was synthesised by layering method. **LP6** (44 mg, 0.1 mmol) was taken in DMF (4 mL), MeOH (9 mL) and layered over aqueous solution of Cu(NO $_3$) $_2$ (2 mL, 24.6 mg, 0.1 mmol). After four weeks light blue, plate shaped crystals were obtained. Elemental analysis (calcd (found) %) for C, 46.85 (46.39), H, 4.75 (4.39), N, 15.93 (15.90) %; FT-IR (KBr, cm $^{-1}$): $\tilde{\nu}= 3339$ (brs, urea N-H stretch), 1716 (s, urea C=O stretch), (see the Supporting Information, Figure S5)

Scanning Electron Microscopy:

Gelatinous precipitate of **LP6** in DMSO/H $_2$ O and **CP3** in DMSO/H $_2$ O were drop casted on glass plated metallic stub and dried under ambient conditions. Next the samples were coated with platinum, and the SEM images were recorded.

Transmission Electron Microscopy.

Small amount of gel sample was smeared on a carbon-coated Cu grid (300 mesh), dried under vacuum at room temperature for 1 d and TEM images were recorded at an accelerating voltage of 200 kV without any staining.

Single-crystal X-ray crystallography

Suitable crystals were isolated, taken in paratone oil and mounted on a glass fibre. The data were collected using Mo K α ($\lambda= 0.7107 \text{ \AA}$) radiation on a BRUKER APEX II diffractometer equipped with CCD area detector. Data collection and data reduction were carried out using the software package APEX II on routine manner. The structure was solved by direct method and refined by full-matrix least-squares based on F 2 values against all reflections in SHELXL-2014 suite of APEX II. Data for **CP5** were collected in a Bruker D8VENTURE Microfocus diffractometer

equipped with PHOTON II Detector (Mo_{Kα} radiation, $\lambda = 0.7107 \text{ \AA}$), controlled by the APEX3 (v2017.3-0) software package. Data collection and data reduction were carried out using the software package APEX3 on a routine manner. The structure was solved by direct method and refined by full-matrix least-squares based on F^2 values against all reflections in SHELXL-2014 suite of APEX3. Final refinement and CIF finalisation were carried out in OLEX2 version 1.2.8. The crystal structure of CP6 was found to be merohedrally twin (refined twin component of 0.288(5), 0.712(5)). All the nonhydrogen atoms were treated anisotropically whereas most of the hydrogen atoms were geometrically fixed; wherever possible, the hydrogen atoms associated with guest solvents were located on difference Fourier map and refined. Ortep3 was used to generate the thermal ellipsoid plots. Final CIFs were deposited to CCDC; CCDC no 1824071 (LP6) 1824068 (CP1) 1824065 (CP2) 1824070 (CP3) 1824067 (CP4) 1824066 (CP5) 1824069 (CP6). These data can be obtained free of charge via www.ccdc.cam.ac.uk/data_request/cif (or from the Cambridge Crystallographic Data Centre, 12 Union Road, Cambridge CB21EZ, UK; fax: (+44) 1223-336-033; or deposit@ccdc.cam.ac.uk).

Powder X-ray diffraction

PXRD data were collected using Bruker AXS D8 Advance powder diffractometer (Cu_{Kα1} radiation, $\lambda = 1.5406 \text{ \AA}$) equipped with super speed LYNXEYE detector with a scan speed of 0.2 sec/step (step size = 0.028 ° 2 θ) for the scan range of 2 θ (5°–35°). The sample for data collection was prepared by making a thin film of finely powdered sample (~20 mg) over a glass slide.

Acknowledgements

P. B. and S. G. thank Indian Association for the Cultivation of Science, Kolkata for a research fellowship. PB also thanks Dr. Ahmed Hussain for fruitful discussion in crystal structure refinement. P.D. thanks the Department of Science & Technology, New Delhi, for financial support. Single-crystal X-ray diffraction data were collected at the Department of Biotechnology (DBT)-funded X-ray diffraction facility under the Centres of Excellence and Innovation in Biotechnology (CEIB) program in the Department of Organic Chemistry, IACS, Kolkata.

Keywords: supramolecular gels; nanoparticles; coordination polymers; crystal engineering; stimuli-responsive gels.

- [1] P. Terech, R. G. Weiss, *Chem. Rev.* **1997**, *97*, 3133–3160.
- [2] R. G. Weiss, *J. Am. Chem. Soc.* **2014**, *136*, 7519–7530.
- [3] D. K. Smith, *Nat. Chem.* **2010**, *2*, 162–163.
- [4] E. R. Draper, D. J. Adams, *Chem. Soc. Rev.* **2018**, DOI 10.1039/C7CS00804J.
- [5] F. M. Menger, K. L. Caran, *J. Am. Chem. Soc.* **2000**, *122*, 11679–11691.
- [6] J. H. Jung, M. Park, S. Shinkai, *Chem. Soc. Rev.* **2010**, *39*, 4286–4302.
- [7] P. Dastidar, *Chem. Soc. Rev.* **2008**, *37*, 2699–2715.
- [8] M. Suzuki, K. Hanabusa, *Chem. Soc. Rev.* **2009**, *38*, 967–975.
- [9] S. S. Babu, V. K. Praveen, A. Ajayaghosh, *Chem. Rev.* **2014**, *114*, 1973–2129.
- [10] J. W. Steed, *Chem. Soc. Rev.* **2010**, *39*, 3686–3699.
- [11] M. D. Segarra-Maset, V. J. Nebot, J. F. Miravet, B. Escuder, *Chem. Soc. Rev.* **2013**, *42*, 7086–7098.
- [12] J. H. Van Esch, B. L. Feringa, *Angew. Chem. Int. Ed.* **2000**, *39*, 2263–2266.
- [13] K. N. King, A. J. McNeil, *Chem. Commun.* **2010**, *46*, 3511–3513.
- [14] D. Díaz Díaz, D. Kühbeck, R. J. Koopmans, *Chem. Soc. Rev.* **2011**, *40*, 427–448.
- [15] R. D. Mukhopadhyay, G. Das, A. Ajayaghosh, *Nat. Commun.* **2018**, *9*, 1–9.
- [16] S. Ghosh, V. K. Praveen, A. Ajayaghosh, *Annu. Rev. Mater. Res.* **2016**, *46*, 235–262.
- [17] A. Ajayaghosh, V. K. Praveen, C. Vijayakumar, *Chem. Soc. Rev.* **2008**, *37*, 109–122.
- [18] Y. R. Liu, L. He, J. Zhang, X. Wang, C. Y. Su, *Chem. Mater.* **2009**, *21*, 557–563.
- [19] A. Döring, W. Birnbaum, D. Kuckling, *Chem. Soc. Rev.* **2013**, *42*, 7391–7420.
- [20] B. Escuder, F. Rodríguez-Llansola, J. F. Miravet, *New J. Chem.* **2010**, *34*, 1044–1224.
- [21] J.-S. Shen, Y.-L. Chen, J.-L. Huang, J.-D. Chen, C. Zhao, Y.-Q. Zheng, T. Yu, Y. Yang, H.-W. Zhang, *Soft Matter* **2013**, *9*, 2017–2023.
- [22] K. J. C. Van Bommel, A. Friggeri, S. Shinkai, *Angew. Chem. Int. Ed.* **2003**, *42*, 980–999.
- [23] M.-O. M. Piepenbrock, N. Clarke, J. W. Steed, *Soft Matter* **2011**, *7*, 2412–2418.
- [24] P. K. Vemula, U. Aslam, V. A. Mallia, G. John, *Chem. Mater.* **2007**, *19*, 138–140.
- [25] J. V. Herrikhuyzen, S. J. George, M. R. J. Vos, N. A. J. M. Sommerdijk, A. Ajayaghosh, S. C. J. Meskers, A. P. H. J. Schenning, *Angew. Chem. Int. Ed.* **2007**, *46*, 1825–1828.
- [26] L. Zhu, X. Li, S. Wu, K. T. Nguyen, H. Yan, H. Ågren, Y. Zhao, *J. Am. Chem. Soc.* **2013**, *135*, 9174–9180.
- [27] B. O. Okesola, D. K. Smith, *Chem. Commun.* **2013**, *49*, 11164–11166.
- [28] J. Bachl, S. Oehm, J. Mayr, C. Cativiela, J. J. Marrero-Tellado, D. D. Díaz, *Int. J. Mol. Sci.* **2015**, *16*, 11766–11784.
- [29] J. Majumder, P. Dastidar, *Chem. Eur. J.* **2016**, *22*, 9267–9276.
- [30] D. R. Trivedi, P. Dastidar, *Chem. Mater.* **2006**, *18*, 1470–1478.
- [31] S. Bhattacharya, Y. K. Ghosh, *Chem. Commun.* **2001**, 185–186.
- [32] E. Carretti, M. Bonini, L. Dei, B. H. Berrie, *Accounts Chem.* **2010**, *43*, 751–760.
- [33] E. Carretti, E. Fratini, D. Berti, L. Dei, P. Baglioni, *Angew. Chem. Int. Ed.* **2009**, *48*, 8966–8969.
- [34] K. Murata, M. Aoki, T. Nishi, A. Ikeda, S. Shinkai, *J. Chem. Soc. Chem. Commun.* **1991**, 1715–1718.
- [35] B. L. Feringa, J. J. D. de Jong, L. N. Lucas, R. M. Kellogg, J. H. van Esch, *Science* **2004**, *304*, 278–281.
- [36] K. K. Kartha, A. Sandeep, V. K. Praveen, A. Ajayaghosh, *Chem. Rec.* **2015**, *15*, 252–262.
- [37] A. R. Hirst, B. Escuder, J. F. Miravet, D. K. Smith, *Angew. Chem. Int. Ed.* **2008**, *47*, 8002–8018.
- [38] A. V. Kabanov, S. V. Vinogradov, *Angew. Chem. Int. Ed.* **2009**, *48*, 5418–5429.
- [39] F. Zhao, M. L. Ma, B. Xu, *Chem. Soc. Rev.* **2009**, *38*, 883–891.
- [40] J. Majumder, J. Deb, M. R. Das, S. S. Jana, P. Dastidar, *Chem. Commun.* **2014**, *50*, 1671–1674.
- [41] K. Y. Lee, M. C. Peters, K. W. Anderson, D. J. Mooney, *Nature* **2000**, *408*, 998–1000.
- [42] K. Y. Lee, D. J. Mooney, *Chem. Rev.* **2001**, *101*, 1869–1879.
- [43] B. Xing, M.-F. Choi, B. Xu, *Chem. Commun.* **2002**, 362–363.
- [44] A. Y.-Y. Tam, V. W.-W. Yam, *Chem. Soc. Rev.* **2013**, *42*, 1540–1567.
- [45] T. Feldner, M. Häring, S. Saha, J. Esquena, R. Banerjee, D. D. Díaz, *Chem. Mater.* **2016**, *28*, 3210–3217.
- [46] K. Hanabusa, Y. Maesaka, M. Suzuki, M. Kimura, H. Shirai, *Chem. Lett.* **2000**, *29*, 1168–1169.
- [47] D. López, J. M. Guenet, *Macromolecules* **2001**, *34*, 1076–1081.
- [48] T. Ishi-i, R. Iguchi, E. Snip, M. Ikeda, S. Shinkai, *Langmuir* **2001**, *17*, 5825–5833.
- [49] M. Kimura, T. Muto, H. Takimoto, K. Wada, K. Ohta, K. Hanabusa, H. Shirai, N. Kobayashi, *Langmuir* **2000**, *16*, 2078–2082.

- [50] T. Tu, W. Fang, X. Bao, X. Li, K. H. Dötz, *Angew. Chem. Int. Ed.* **2011**, *50*, 6601–6605.
- [51] Q. Wei, S. L. James, *Chem. Commun.* **2005**, 1555–1556.
- [52] B. S. Luisi, K. D. Rowland, B. Moulton, *Chem. Commun.* **2007**, 2802–2804.
- [53] J. Zhang, C. Y. Su, *Coord. Chem. Rev.* **2013**, *257*, 1373–1408.
- [54] J. L. Li, X. Y. Liu, *Adv. Funct. Mater.* **2010**, *20*, 3196–3216.
- [55] Y. Lan, M. G. Corradini, R. G. Weiss, S. R. Raghavan, M. A. Rogers, *Chem. Soc. Rev.* **2015**, *44*, 6035–6058.
- [56] N. N. Adarsh, D. K. Kumar, P. Dastidar, *Tetrahedron* **2007**, *63*, 7386–7396.
- [57] D. K. Kumar, D. A. Jose, A. Das, P. Dastidar, *Chem. Commun.* **2005**, 4059–4061.
- [58] D. K. Kumar, D. A. Jose, P. Dastidar, A. Das, *Chem. Mater.* **2004**, *16*, 2332–2335.
- [59] O. Lebel, M. É. Perron, T. Maris, S. F. Zalzal, A. Nanci, J. D. Wuest, *Chem. Mater.* **2006**, *18*, 3616–3626.
- [60] N. N. Adarsh, P. Sahoo, P. Dastidar, *Cryst. Growth Des.* **2010**, *10*, 4976–4986.
- [61] N. N. Adarsh, P. Dastidar, *Cryst. Growth Des.* **2011**, *11*, 328–336.
- [62] P. Dastidar, S. Ganguly, K. Sarkar, *Chem. Asian. J.* **2016**, *11*, 2484–2498.
- [63] D. B. Grotjahn, C. Joubran, *Tetrahedron: Asymmetry* **1995**, *6*, 745–752.
- [64] E. Bash, *Dalton. Trans.* **2003**, *1*, 3339–3349.
- [65] E. V. Alexandrov, V. A. Blatov, A. V. Kochetkov, D. M. Proserpio, *CrystEngComm* **2011**, *13*, 3947–3958.
- [66] V. A. Blatov, *Struct. Chem.* **2012**, *23*, 955–963.
- [67] M. Paul, K. Sarkar, P. Dastidar, *Chem. Eur. J.* **2015**, *21*, 255–268.
- [68] H. Basit, A. Pal, S. Sen, S. Bhattacharya, *Chem. Eur. J.* **2008**, *14*, 6534–6545.
- [69] J. Young Yook, G.-H. Choi, D. Hack Suh, *Chem. Commun.* **2012**, *48*, 5001.
- [70] R. A. Agarwal *Sci. Rep.* **2017**, *7*, 1–9.
- [71] S. R. Raghavan, M. W. Riley, P. S. Fedkiw, S. A. Khan, *Chem. Mater.* **1998**, *10*, 244–251.
- [72] M. L. H.-J. Kim, J.-H. Lee, *Angew. Chem. Int. Ed.* **2005**, *117*, 5960–5964.
- [73] J. E. A. Webb, M. J. Crossley, P. Turner, P. Thordarson, *J. Am. Chem. Soc.* **2007**, *129*, 7155–7162.
- [74] N. H. Andersen, P. Chen, Q. Li, S. Grindy, *J. Am. Chem. Soc.* **2015**, *137*, 11590–11593.

Table 1: Crystal data

Identification code	LP6	CP1	CP2	CP3	CP4	CP5	CP6
Empirical formula	C ₄₈ H ₄₀ N ₁₂ O ₆	C ₂₄ H ₂₂ Cl ₂ N ₆ O ₄ Zn	C ₂₄ H ₂₂ N ₆ O ₈ SZn	C ₄₉ H ₅₀ F ₆ N ₁₂ O ₁₁ SiZn	C ₂₄ H ₂₀ AgClN ₆ O ₇	C ₃₀ H ₃₄ AgBF ₄ N ₈ O ₅	C ₄₈ H ₄₇ CuN ₁₄ O ₁₉
Formula weight	880.92	594.74	619.90	1190.47	647.78	781.33	1187.53
Temperature/K	296.15	293.15	296.15	119.82	296.15	114.0	296.15
Crystal system	monoclinic	orthorhombic	triclinic	triclinic	monoclinic	triclinic	tetragonal
Space group	P2 ₁	Pca2 ₁	P-1	P1	C2/c	P-1	P4 ₂
a/Å	6.2025(12)	12.1733(8)	7.205(4)	7.434(8)	25.5465(9)	6.603(2)	18.421(13)
b/Å	44.576(8)	24.8750(16)	12.795(8)	13.743(16)	9.4070(4)	13.211(5)	18.421(13)
c/Å	7.4081(13)	8.2976(6)	14.006(9)	14.672(16)	22.5479(8)	19.318(5)	16.754(12)
α°	90	90	90.506(9)	62.595(11)	90	75.785(6)	90
β°	94.397(5)	90	94.623(9)	82.914(12)	114.363(2)	85.080(10)	90
γ°	90	90	92.126(9)	85.872(12)	90	84.090(10)	90
Volume/Å ³	2042.2(7)	2512.6(3)	1286.2(14)	1320(3)	4936.1(3)	1621.7(9)	5685(9)
Z	2	4	2	1	8	2	4
ρ _{calc} /cm ³	1.433	1.572	1.601	1.497	1.743	1.600	1.387
μ/mm ⁻¹	0.099	1.234	1.098	0.581	0.984	0.698	0.468
F(000)	920.0	1216.0	636.0	614.0	2608.0	796.0	2456.0
Crystal size/mm ³	0.38 × 0.35 × 0.3	0.42 × 0.32 × 0.3	0.41 × 0.3 × 0.24	0.41 × 0.3 × 0.24	0.35 × 0.26 × 0.2	0.23 × 0.2 × 0.09	0.2 × 0.15 × 0.14
Radiation	MoKα (λ = 0.71073)	MoKα (λ = 0.71073)	MoKα (λ = 0.71073)	MoKα (λ = 0.71073)	MoKα (λ = 0.71073)	MoKα (λ = 0.71073)	MoKα (λ = 0.71073)
2θ range for data collection/°	3.654 to 43.664	3.274 to 51.338	2.918 to 52.394	3.144 to 49.462	3.966 to 51.468	4.358 to 50.908	2.21 to 45.094
Index ranges	-6 ≤ h ≤ 6, -45 ≤ k ≤ 45, -7 ≤ l ≤ 7	-14 ≤ h ≤ 14, -30 ≤ k ≤ 30, -9 ≤ l ≤ 10	-8 ≤ h ≤ 8, -15 ≤ k ≤ 15, -17 ≤ l ≤ 17	-8 ≤ h ≤ 8, -15 ≤ k ≤ 15, -16 ≤ l ≤ 16	-31 ≤ h ≤ 30, -11 ≤ k ≤ 11, -26 ≤ l ≤ 27	-7 ≤ h ≤ 7, -15 ≤ k ≤ 15, -21 ≤ l ≤ 23	-19 ≤ h ≤ 19, -17 ≤ k ≤ 19, -17 ≤ l ≤ 17
Reflections collected	12137	30794	24737	17869	22842	15311	47657
Independent reflections	3987 [R _{int} = 0.0746, R _{sigma} = 0.0854]	4655 [R _{int} = 0.1435, R _{sigma} = 0.1080]	5120 [R _{int} = 0.1015, R _{sigma} = 0.0905]	8450 [R _{int} = 0.0571, R _{sigma} = 0.0974]	4704 [R _{int} = 0.0473, R _{sigma} = 0.0396]	5895 [R _{int} = 0.1088, R _{sigma} = 0.1740]	7415 [R _{int} = 0.1501, R _{sigma} = 0.1094]
Data/restraints/parameters	3987/1/596	4655/1/337	5120/0/362	8450/3/728	4704/89/360	5895/0/446	7415/1221/740
Goodness-of-fit on F ²	1.080	1.019	0.977	1.018	1.047	1.104	1.042
Final R indexes [I > 2σ(I)]	R ₁ = 0.0595, wR ₂ = 0.1265	R ₁ = 0.0543, wR ₂ = 0.1007	R ₁ = 0.0507, wR ₂ = 0.1148	R ₁ = 0.0528, wR ₂ = 0.1281	R ₁ = 0.0618, wR ₂ = 0.1588	R ₁ = 0.1065, wR ₂ = 0.2512	R ₁ = 0.0883, wR ₂ = 0.2227
Final R indexes [all data]	R ₁ = 0.0795, wR ₂ = 0.1525	R ₁ = 0.0920, wR ₂ = 0.1175	R ₁ = 0.1086, wR ₂ = 0.1475	R ₁ = 0.0827, wR ₂ = 0.1650	R ₁ = 0.0868, wR ₂ = 0.1772	R ₁ = 0.1971, wR ₂ = 0.2942	R ₁ = 0.1313, wR ₂ = 0.2575
Largest diff. peak/hole /	0.57/-0.39	0.40/-0.42	0.51/-0.62	0.52/-0.79	2.02/-2.23	1.78/-1.41	1.14/-0.53

e Å ⁻³							
-------------------	--	--	--	--	--	--	--

Table 2: Gelation table of various metal salts.

Metallogels	Metal salt	LP6 / Metal salt (mg) (1:1 molar ratio)	DMSO: H ₂ O (2:3)	MGC (wt %)
CPMG1	ZnCl ₂	4.5 mg / 1.40 mg	1mL	4.5
CPMG2	ZnSO ₄	4.5 mg / 1.67 mg	1mL	4.5
CPMG4	AgClO ₄	5.5 mg / 2.59 mg	1mL	5.5
CPMG5	AgBF ₄	5.0 mg / 2.20 mg	1mL	5.0
CPMG6	Cu(NO ₃) ₂	4.5 mg / 1.93 mg	1mL	4.5
MG7	CuCl ₂	3.5 mg / 1.06 mg	1mL	3.5
MG8	NiCl ₂	5.0 mg / 1.48 mg	1mL	5.0
MG9	CoCl ₂	4.5 mg / 1.32 mg	1mL	4.5
MG10	CdCl ₂	6.5 mg / 2.70 mg	1mL	6.5
MG11	NaCl	7.5 mg / 1.96 mg*	1mL	7.5
MG12	MnCl ₂	5.5 mg / 1.58 mg	1mL	5.5

* 2:1 metal salt:LP6

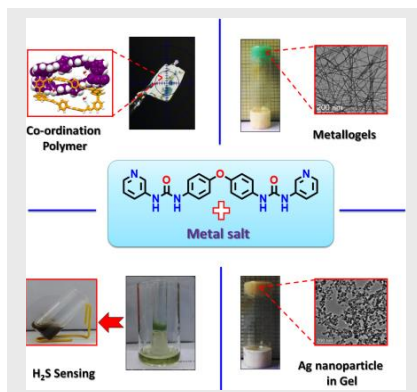
Table 3: Rheology table for various metallogels.

Metallogels	Average G' (KPa)	Average G'' (KPa)	G''/ G'
CPMG1	23.6	3.1	0.129
CPMG2	53.8	6.9	0.130
CPMG4	23.0	5.3	0.230
CPMG5	5.3	0.5	0.102
CPMG6	10.9	1.2	0.114
MG7	100.1	9.9	0.099
MG8	14.8	0.7	0.050
MG9	17.2	2.2	0.128
MG10	3.7	0.3	0.039
MG11	0.7	0.1	0.107

Entry for the Table of Contents.

FULL PAPER

Exploiting crystal engineering aspects, a series of coordination polymers derived from a bis-pyridyl-bis-urea ligand was designed; the corresponding metallogels displayed the ability to produce Ag nanoparticle and sense hazardous gases.



*Protap Biswas, Sumi Ganguly,
Parthasarathi Dastidar**

Page No. – Page No.

**Stimuli-responsive Metallogels for
synthesizing Ag nanoparticles and
Sensing Hazardous Gases**